FEBS Letters 523 (2002) 152–156 FEBS 26264

Direct evidence for alteration of unfolding profile of a helical peptide by far-ultraviolet circular dichroism aromatic side-chain contribution

Raja Banerjee[1], Gautam Basu*

Department of Biophysics, Bose Institute, P-1/12 CIT Scheme VIIM, Calcutta 700 054, India

Received 23 January 2002; revised 11 June 2002; accepted 12 June 2002

First published online 25 June 2002

Edited by Hans Eklund

Abstract Aromatic side-chains are known to contribute to the far-UV circular dichroism (CD) spectra of peptides and proteins. Among other things, this can significantly affect the measured helix propensities of amino acids [Chakrabartty et al., Biochemistry 32 (1993) 5560–5565]. In order to address how interfering side-chain contributions can affect the backbone unfolding transition of a helical peptide, as monitored by $[\theta]_{222}$ (molar ellipticity at 222 nm), we have studied the unfolding transition of a short designed (α-amino isobutyric acid/alanine-based) helical peptide containing an interacting Tyr residue. The guanidinium hydrochloride-induced unfolding of the peptide, as monitored by $[\theta]_{222}$, showed the presence of a sharp transition superposed over a much broader transition. When the same experiment was performed with a similar peptide that lacked the interacting Tyr residue, the sharp transition disappeared and only the broad transition remained. The sharp transition was assigned to originate from the interacting Tyr side-chain. This demonstrates that conformationally restricted aromatic side-chains that interact with the helical backbone not only can alter the backbone far-UV CD signal, they may also alter the unfolding profiles, monitored by far-UV CD, rendering them unfit for a simple analysis for extracting the appropriate unfolding thermodynamic parameters.

Key words: Circular dichroism; α-Amino isobutyric acid; Helix; Peptide unfolding; Tyrosine

1. Introduction

Far-ultraviolet circular dichroism (far-UV CD) spectroscopy is a powerful tool that can provide information about the secondary structural content of a polypeptide chain [1]. In fact the technique is the most direct way of probing the secondary structural content of a protein in solution within a reasonable error margin. The far-UV CD spectrum originates primarily from the asymmetric juxtaposition of the backbone amide groups of the peptide chain in the folded state [2]. When unfolded, the compact structure of the interacting amide groups gets disrupted, thus diminishing the far-UV CD signature. This dramatic difference of far-UV CD signal between the folded and the unfolded states of a protein is the reason why it is the method of choice for monitoring protein unfolding [3].

However, backbone amide groups may not be the sole contributor to the observed far-UV CD signal of a folded polypeptide chain. Contributions from side-chain chromophores, especially Phe, Tyr and Trp, can potentially alter the overall far-UV CD signal if they are locked in asymmetric geometries as well, arising from favorable interaction with the backbone. This phenomenon is well known in proteins [4] and was unequivocally pointed out to be operating in small designed helical peptides [5]. In order to assess how interfering side-chain contributions can alter the far-UV CD-monitored backbone unfolding profile of polypeptide chains, we have studied the guanidine hydrochloride (GnCl)-induced unfolding of a 12 residue peptide containing three α-amino isobutyric acid (Aib) residues, a strong helix promoter [6–9]. The sequence contained a Tyr residue at its C-terminal whose side-chain can potentially interact with the core peptide helix. The unfolding profile of this peptide was then compared with that of a similar peptide where the C-terminal Tyr is conformationally disconnected from the core peptide helix by two helix-breaker Gly residues. The difference in the two unfolding profiles allowed us to directly probe the contribution of the Tyr side-chain in the far-UV CD-monitored unfolding profile of the 12 residue peptide. Implications of the results are discussed.

2. Materials and methods

2.1. Peptide synthesis and characterization

The sequences of the designed peptides used in this study are: (i) ABK: Ac-Ala-Aib-Ala-Lys-Ala-Aib-Lys-Ala-Lys-Ala-Aib-Tyr-NH_2, and (ii) ABGY: Ac-Ala-Aib-Ala-Lys-Ala-Aib-Lys-Ala-Lys-Ala-Aib-Gly-Gly-Tyr-NH_2. Both peptides were synthesized via Fmoc chemistry on a solid phase Rink amide MBHA resin on a semiautomatic Biolynx 4175 LKB peptide synthesizer. Aib residues were added as N-protected free acids along with HOBT, PyBOP and DIPEA while all other amino acids were added as N-protected Opfp esters along with HOBT. N-terminal acetylation was achieved by acetic anhydride and triethylamine in dimethylfluoride prior to detaching the growing peptide from the resin by 95% trifluoroacetic acid (TFA). The crude peptides were subjected to high performance liquid chromatography on a C18 ODS2 column and purified by using 0–60% CH_3CN/H_2O (0.1% TFA) gradient. The peptides were fully characterized by ^{1}H-nuclear magnetic spectroscopy (NMR).

2.2. ^{1}H-NMR and CD spectroscopy

All ^{1}H-NMR experiments were performed on a Bruker DRX 500 MHz spectrometer. Samples were prepared in 10 mM phosphate buffer (pH 3.1) containing 10% D_2O [v/v] and 1 M NaCl with TSP as the internal standard. Water suppression was achieved using WATERGATE pulse sequence [10] for all experiments. TOCSY [11] and ROESY [12] experiments were performed using standard protocols [13].

*Corresponding author.
E-mail address: gautam@boseinst.ernet.in (G. Basu).

[1] Permanent address: Department of Chemistry, St. Xavier's College, Calcutta 700016, India.

0014-5793/02/$22.00
PII: S0014-5793(02)02974-5

Far-UV CD spectra were recorded at 25°C in a JASCO J-600 spectropolarimeter in 1 and 2 mm pathlength cuvettes. The bandwidth was 1 nm and scan speed was 20 nm/min. Samples were prepared in 10 mM phosphate buffer (pH 3.1) with peptide concentrations being approximately 60 μM in the presence of 1 M NaCl. Peptide concentrations were calculated from Tyr absorbance at 275 nm ($\varepsilon = 1450$ cm^{-1} M^{-1}) and used in calculating mean residue ellipticities [θ]. Fraction helicity (f_H) values were estimated [1] as

$$f_H = [\theta]^{obs}_{222}/(-40000 \pm 2500)\left(1-\frac{k_\lambda}{n}\right) \quad (1)$$

where n is the number of residues, k_λ is a wavelength-dependent constant (2.5 at 222 nm) and $[\theta]^{obs}_{222}$ is the observed [θ] at 222 nm.

2.3. Analysis of unfolding data

GnCl-induced unfolding transition profiles were analyzed with a two-state

$$[\theta]^{obs}_{222} = \frac{[\theta]^{U}_{222} + [\theta]^{F}_{222}\exp\{\Delta G_{FU}(d)/RT\}}{1+\exp\{\Delta G_{FU}(d)/RT\}} \quad (2)$$

or a three-state equation

$$[\theta]^{obs}_{222} = \frac{[\theta]^{U}_{222} + [\theta]^{F}_{222}\exp\{\Delta G_{FU}(d)/RT\} + [\theta]^{I}_{222}\exp\{\Delta G_{IU}(d)/RT\}}{1+\exp\{\Delta G_{FU}(d)/RT\}+\exp\{\Delta G_{IU}(d)/RT\}} \quad (3)$$

where $[\theta]^{U}_{222}$, $[\theta]^{F}_{222}$ and $[\theta]^{I}_{222}$ correspond to the limiting $[\theta]_{222}$ values of the unfolded (U), folded (F) and the mandatory intermediate (I) states respectively. The free energies, ΔG_{FU} and ΔG_{IU} were assumed to depend linearly on denaturant concentration [d] as

$$\Delta G_{FU}(d) = \Delta G^{H2O}_{FU} - m_{FU}[d]$$
$$\Delta G_{IU}(d) = \Delta G^{H2O}_{IU} - m_{IU}[d] \quad (4)$$

where the superscript H2O indicates free energies in the absence of denaturant.

3. Results and discussion

3.1. Peptide design

The peptides used in this work, ABK and ABGY, were designed to be helical and water-soluble. For inducing helicity, apart from incorporation of the Ala residues, three Aib residues were incorporated for their proven ability to stabilize the helical backbone [6–9]. We also wanted the peptides to be short (about 12 residues), so that they are amenable to ^{1}H-NMR studies, and yet show considerable helicity at ambient temperature, so that their conformational properties need not be valid only at near 0°C, as is the case with most synthetic helical peptides [14]. Aib was chosen to address these points as well. The purpose of the three Lys residues, placed in the sequence in a manner such that they span out radially around a helical backbone, was to prevent aggregation and increase solubility. The Tyr residue, introduced for precise measurement of peptide concentration, is conformationally disconnected from the core helix by two Gly residues in ABGY [5]. In summary, both ABK and ABGY share almost identical sequences and were designed to be helical at ambient temperature. However, while the terminal Tyr in ABK can potentially interact with the helical peptide backbone, in ABGY such interactions are very unlikely.

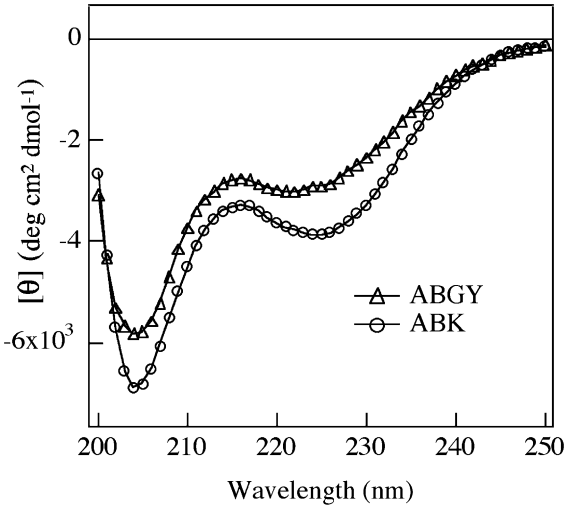

Fig. 1. The far-UV CD spectra of ABGY (top) and ABK (bottom) (pH 3.1, 10 mM phosphate buffer, 1 M NaCl) at 25°C. Both spectra show a helix-like double minimum but the intensities are far less than expected.

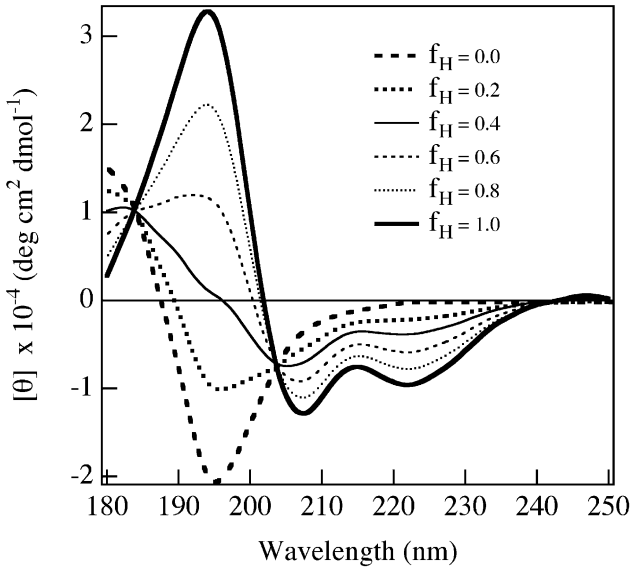

Fig. 2. The far-UV CD spectra of a polypeptide backbone generated as a function of fraction helicity (f_H) in a two-state model (helix and coil) using base spectra reported by Obrecht et al. [16]. The characteristic $\pi\pi^*_{\parallel}$ minimum, corresponding to the helix, begins to appear beyond 203 nm only at greater than 30% f_H values.

3.2. CD studies

Far-UV CD spectra of ABK and ABGY are shown in Fig. 1. Both show the characteristic double minimum (208–210 and 222 nm) associated with polypeptide helices [1], although their exact positions are slightly different (~205 and 224–225 nm). Compared to ABK, the reduced CD signal (absolute intensity) of ABGY is expected, since ABGY contains two extra Gly residues. However, since the CD signal of ABK has the possibility of potential interference from the Tyr side-chain, interpretation of the difference is not straightforward. In fact, Baldwin and co-workers [5], from their analysis of a series of helical peptides, with and without side-chain contribution, had suggested that the presence of an interacting Tyr side-chain changes $[\theta]_{222}$ by 4400 ± 1000 deg cm^2 dmol^{-1}. If indeed that is the case here, the corrected $[\theta]^{ABK}_{222}$ (-3770–4400 ± 1000 deg cm^2 dmol^{-1}) is more than twice that of $[\theta]^{ABGY}_{222}$ (-3010 deg cm^2 dmol^{-1}). Clearly that cannot be true since $[\theta]^{ABK}_{222}$, after correction for the Tyr contribution, is expected to be only slightly stronger than $[\theta]^{ABGY}_{222}$, chiefly due to the two extra Gly residues in ABGY. Therefore, the actual aromatic side-chain contribution from the Tyr side-

chain in ABK must be much smaller than what has been suggested for Ala-based helices [5].

Fraction helicity of the peptides, estimated according to Eq. 1, yielded $f_H^{ABGY} = 0.09$ and $f_H^{ABK} = 0.12$ (uncorrected). Although the exact value of k_λ (we used 2.5) in Eq. 1 for calculating f_H has been under scrutiny, even using the range of alternative values of k_λ [15] predicts the peptides to be only nominally helical. The estimated f_H^{ABGY} and f_{ABK}^H values cannot be correct as illustrated here by a simple argument. Eq. 1 assumes a two-state system (completely helical and completely random, where the latter has no $[\theta]_{222}$ contribution). Therefore, a knowledge of the far-UV CD spectra for the two base states should enable one to reconstruct the far-UV CD spectrum corresponding to f_H values predicted by Eq. 1. In Fig. 2 we show a series of spectra corresponding to $f_H = 0.0$, 0.2, 0.4, 0.6, 0.8 and 1.0 using reported α-helix and coil base spectra [16]. As can be seen from Fig. 2, the effective position of the $\pi\pi^*_{\parallel}$ minimum from the helix appears ≥ 203 nm only at $f_H > 0.3$. For both ABK and ABGY, the position of the $\pi\pi^*_{\parallel}$ minimum appears around 205 nm indicating that they should at least be 30–40% helical. This holds true even if one uses different base spectra [1] for generating f_H-dependent CD spectra [15]. Further support for helical backbone of ABK and ABGY comes from ^{1}H-NMR studies as discussed in Section 3.3.

The relatively low values of $[\theta]_{222}^{ABK}$ and $[\theta]_{222}^{ABGY}$ can arise from several reasons, of which we will mention two here. One possibility is that the far-UV CD spectra of the 'coil' states of ABK and ABGY are different from that of Ala-based peptides. This is because of the presence of the Aib residue, whose allowed conformational space is severely restricted to the helical region only. The other possibility is that Aib-containing ABK and ABGY sequences do not always produce right-handed helices, rather an admixture of the classical right-handed and its mirror image are generated, albeit in unequal proportion. The achiral Aib residues will equally prefer helices of both handedness while the large number of L-amino acids in ABK and ABGY will prefer the right-handed over the left-handed helix. As a result an excess population of the right-handed helix will be produced which will give rise to the observed CD signal, much diminished from that expected from the entire helical population in a right-handed conformation. This is an attractive model that can explain why the far-UV CD contribution from the Tyr residue in ABK is much smaller than the predicted value for Ala-based helices [5]. The actual Tyr contribution from the right-handed and left-handed helices, like the contribution from the backbone amides, will be of opposite sign, resulting in only a small effective contribution arising from the excess population of the right-handed helices only.

3.3. NMR studies

We performed one- and two-dimensional ^{1}H-NMR experiments at 27°C on ABK and ABGY. For ABK, TOCSY experiments allowed us to unambiguously assign the spin systems. The standard αN(i,i+1) and βN(i,i+1) ROE walk (data not shown) was used to sequence assign all residues except Ala3, Ala8, Lys4 and Lys7 (due to severe overlap of C$^\alpha$H resonances), which were subsequently assigned using the NN(i,i+1) ROE walk recommended for peptides with a high percentage of Aib that lack C$^\alpha$H [17]. The implicit assumption in using the NN(i,i+1) ROE walk is that the peptide backbone

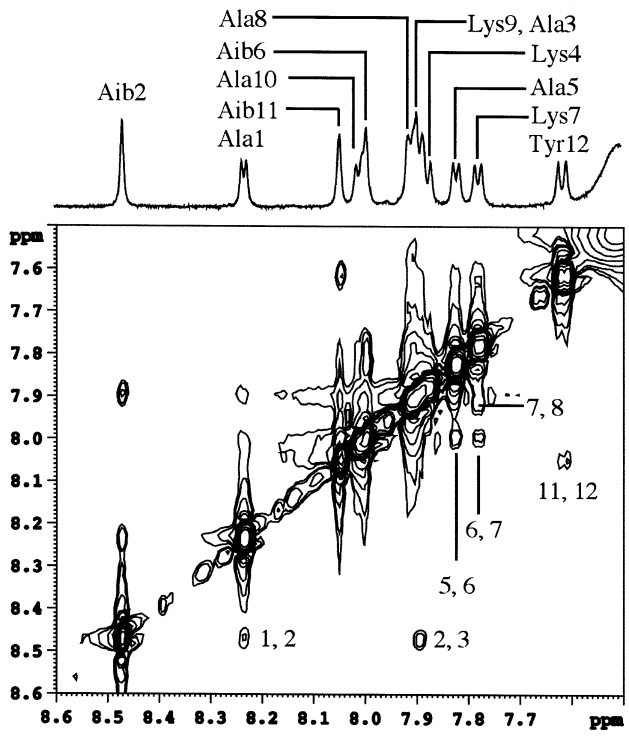

Fig. 3. NN amide region of the ROESY (200 ms mixing time) spectrum of ABK (pH 3.1, 10 mM phosphate buffer, 1 M NaCl) at 27°C. The amide peaks are indicated in the one-dimensional spectrum and all the discernible ROE cross-peaks are sequence labeled.

is helical for which we had independent support from CD data. The NN(i,i+1) ROESY spectrum for ABK at 27°C is given in Fig. 3. Of a total of 11 possible NN(i,i+1) cross-peaks six were observed (Fig. 3) while the unobserved cross-peaks were all too close to the diagonal for unambiguous detection. The observed continuous stretch of NN(i,i+1) cross-peaks characterizes a helical backbone [18]. The αN(i,i) cross-peaks were comparable to or stronger than the αN(i,i+1) cross-peaks for most of the residues further supporting a helical backbone [18]. αN(i,i+3) or αN(i,i+4) cross-peaks, characteristic of a helix, were not observed, chiefly due to spectral overlap or to their weak nature. The select set of $^3J_{N\alpha}$ values that could be measured from the 1D spectra was small and supported [18] a helical backbone as well (Ala1: 4.4 Hz, Ala5: 5.1 Hz, Lys7: 6.0 Hz, Ala10: 5.1 Hz). It is well known that the C$^\alpha$H resonances of residues, when present in a helical conformation, are typically upfield shifted compared to when present in unordered conformation [19]. Chemical shift index (CSI) values, the difference in ^{1}H-NMR chemical shift values of C$^\alpha$H protons from the random coil values, for ABK are shown in Fig. 4, which shows consistent C$^\alpha$H upfield shifts of more than 0.1 ppm indicating the presence of helical backbone [19]. An analysis of the NN ROESY spectrum of ABGY showed cross-peaks very similar to ABK. The CSI values of ABGY are shown in Fig. 4 for comparison. In summary, from NMR experiments we found both ABK and ABGY to exhibit substantial helicity in solution.

3.4. GnCl-induced unfolding of ABK and ABGY monitored by far-UV CD

Having established that both ABK and ABGY are helical at 27°C in solution, let us now focus on their unfolding prop-

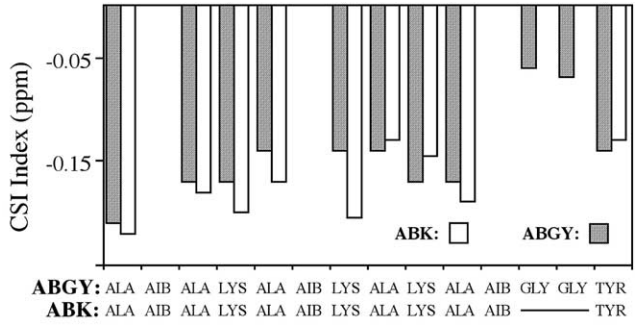

Fig. 4. CSI of ABK and ABGY (pH 3.1, 10 mM phosphate buffer, 1 M NaCl) at 27°C. Except the two Gly residues all residues in both peptides show more than 0.1 ppm upfield shift indicating the presence of helical backbone.

erties. Although unfolding of Ala-based peptide helices has been reported both as a function of temperature [20] and as a function of chaotropic agents like urea [21] and GnCl [22], peptide helices containing a high percentage of Aib residues are usually resistant to thermal unfolding [23]. Both ABK and ABGY showed thermostability up to 60°C as monitored by the change in $^3J_{N\alpha}$ coupling constants. However, both the peptides unfolded in the presence of a high concentration of GnCl. The observed values of values of $[\theta]_{222}^{ABK}$ and $[\theta]_{222}^{ABGY}$ as a function of added GnCl are shown in Fig. 5.

We will first consider the ABGY data. Fig. 5 shows a broad unfolding transition as expected from a short helical peptide. The parameters obtained from a simple two-state (Eq. 2) analysis of the unfolding data are given in Table 1 and the fit is shown in Fig. 5. The analysis assigns a value of 0.69 kcal mol^{-1} to ΔG_{FU}^{H2O}, the free energy difference between the unfolded and the folded states of ABGY, and a value of 0.41 kcal mol^{-1} M^{-1} to m_{FU}. The midpoint of transition is 1.68 M GnCl.

A study of GnCl-induced unfolding of ABK also showed almost similar variation in $[\theta]_{222}^{ABK}$ as in $[\theta]_{222}^{ABGY}$, except that the $[\theta]_{222}^{ABK}$ plateau, upon complete unfolding, is different from that of ABGY. Most importantly, visual inspection of the unfolding profile shows a sharp change in $[\theta]_{222}^{ABK}$ at early GnCl concentrations, over and above the broad transition that was observed for ABGY. The ABK data were analyzed with a two- as well as with a three-state model, the latter included an obligatory intermediate (I) state. Both fits are shown in Fig. 5 and the relevant parameters are given in Table 1. Clearly the two-state model is inadequate for describing the transition curve although the deduced ΔG_{FU}^{H2O} and m_{FU} values are close to those obtained for ABGY (within the reported error margin). The three-state fit, on the other hand, describes the transition well. However, an inspection of the three-state parameters (Table 1) reveals them to be unphysical. For example, it is difficult, if not impossible, to physically attribute a conformational transition in ABK with a free energy change of 6.5 kcal mol^{-1} and a m_{FU} value of 3.4 kcal mol^{-1} M^{-1}.

The primary difference between ABK and ABGY is in the presence of an interacting Tyr in ABK. Therefore we assign the apparent sharp transition in ABK at early GnCl concentrations to be arising from the interacting Tyr residue. The observed kink can, in principle, result from aggregation. However, aggregation can be ruled out from the following considerations: (i) the CD spectra of the peptide were found to be independent of concentration around the range of concentrations used in the CD study, (ii) ABGY, identical in sequence except for the C-termini $(Gly)_2$ insertion, should have shown aggregation and the kink, and (iii) the presence of three Lys side-chains in such a short peptide makes aggregation unlikely. Specific binding of GnCl to the Tyr side-chain, as a mechanism for the observed kink, is also unlikely since any such specific binding to the Tyr side-chain should have affected both ABK and ABGY.

What could then be the origin of the sharp transition? Strictly speaking, the helix–coil transition of short peptides in water is not a two-state transition, due to low helix propagation constants [24]. The same probably applies to ABK and ABGY. In other words, a large number of partially helical (along the sequence, in a contiguous fashion or in isolation) conformations co-exist in equilibrium. It is also known, from computer simulations, that typically a helix starts to melt from its C-terminus [25,26]. One can thus envisage a scenario where, via inter-conversion between the micro-states, the C-terminus of the helix first melts, as a function of increasing GnCl concentration. Complications may arise if there are several unfolding events that are overlapped, and especially if the limiting values of the successive unfolded (partial) micro-states do not change monotonically. As the helix melts, while the absolute value of $[\theta]_{222}^{ABK}$ (backbone), arising from successive micro-states, can only decrease, there is no guarantee that the same is applicable to $[\theta]_{222}^{ABK}$ (Tyr side-chain). The relative intensities of aromatic contribution to $[\theta]_{222}^{ABK}$, in micro-states that allow an interacting Tyr, will depend on the exact geometry of interaction. This will give rise to potential non-monotonic changes in overall limiting values of $[\theta]_{222}^{ABK}$ in the micro-states, after each unfolding event. In such a case, several overlapped unfolding events may result in a final 'effective' single unfolding effect with a physically unrealistic 'effective' m value from a simple three-state analysis. Even if one did a multi-state analysis there will be too many parameters to fit with confidence. That is what we think is happening in the early part of the ABK transition – a physically unrealistic 'effective' m value results from a simple three-state analysis.

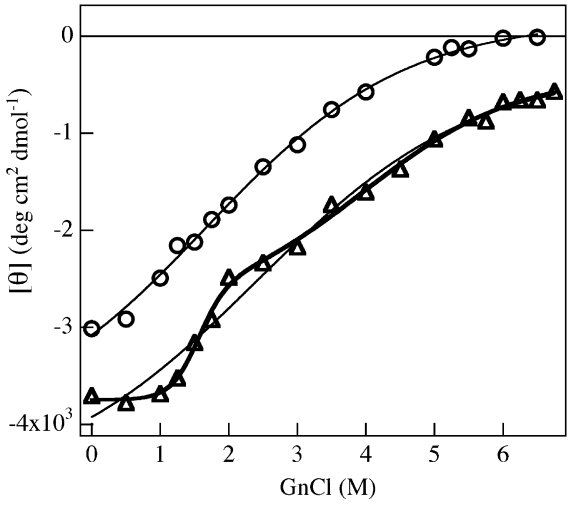

Fig. 5. Variation of mean residue ellipticity of ABGY (○) and ABK (△) as a function of added GnCl at 25°C. The curves are the best fits (Eqs. 2 and 3) to the data and the corresponding parameters are given in Table 1. The heavy curve represents a three-state fit (Eq. 3) while the light curves indicate two-state fits (Eq. 2).

Table 1
Analysis of GnCl-induced unfolding of ABK and ABGY

Fit parameter[a]	Two-state model		Three-state model
	ABGY	ABK	ABK
$[\theta]_{222}^{U}$	165 ± 78[b]	−340 ± 234	−395 ± 165
$[\theta]_{222}^{F}$	−4089 ± 286	−4694 ± 578	−3745 ± 48
$[\theta]_{222}^{I}$	–	–	−2805 ± 412
ΔG_{FU}^{H2O}	0.69 ± 0.16	0.91 ± 0.33	6.53 ± 0.94
m_{FU}	0.41 ± 0.05	0.38 ± 0.09	3.38 ± 0.62
ΔG_{IU}^{H2O}	–	–	2.11 ± 0.75
m_{IU}	–	–	0.53 ± 0.15

[a]The units are: $[\theta]$ values: deg cm^{-1} dmol^{-1}; ΔG values: kcal mol^{-1}; m values: kcal mol^{-1} M^{-1}.
[b]The errors represent standard deviations from the curve fit.

In the model proposed above, the observed anomalous sharp transition at low GnCl concentration is attributed to subtle changes in Tyr side-chain conformation in micro-states involving the C-terminus melting. For low GnCl concentrations, this produces a Tyr side-chain CD signal profile not linearly correlated to any major change of backbone conformation. After the completion of C-terminal melting, the far-UV CD contribution of Tyr reaches a new value. This value is maintained until the end of the transition – the negative $[\theta]_{222}^{ABK}$ plateau, observed at high GnCl concentration. In other words, the Tyr side-chain in ABK not only contributes to the observed far-UV CD spectrum, it also affects the CD-monitored unfolding profile. The interaction of the side-chain with the backbone, which contributes to $[\theta]_{222}^{ABK}$, changes with progressive backbone unfolding in a manner that makes the CD-monitored unfolding curve unreliable for analysis in terms of peptide backbone unfolding.

4. Conclusion

We have designed two Aib containing short peptides which were shown to be helical in aqueous solution, with no added co-solvent, by CD (25°C) and NMR (27°C) spectroscopy. By combining NMR and CD data we showed that the peptides are substantially more helical than predicted from a simple analysis of $[\theta]_{222}^{obs}$ values, possibly due to the presence of unequal populations of helical enantiomers. The two peptides differed in the placement of a terminal Tyr residue – in one (ABK) the Tyr side-chain was allowed to interact with the main helix and in the other (ABGY) it was not. By comparing the far-UV CD spectra of the two peptides, as a function of added GnCl, we showed that there is a small contribution from the Tyr side-chain to the far-UV CD spectrum in ABK. The observed magnitude was much smaller than expected, for the same reason that gave rise to lower than expected values of $[\theta]_{222}^{obs}$. More importantly, we showed that the interacting Tyr in ABK altered the far-UV CD-monitored backbone unfolding profile. This is the central result of this paper and its implications can be far reaching, especially in cases where far-UV CD is used as a tool for monitoring structural changes [3]. It will be interesting to study if the interacting Tyr side-chain also affects interpretation of far-UV CD-monitored backbone unfolding kinetics [27].

Acknowledgements: We would like to thank Jaganmoy Guin, Ashim Banerjee and Barun Majumder for help with the CD, HPLC and NMR experiments. G.B. acknowledges financial support from DST, Government of India, and R.B. acknowledges financial support from UGC, India (under the FIP scheme).

References

[1] Yang, J.T., Wu, C.-S.C. and Martinez, H.M. (1986) Methods Enzymol. 130, 208–269.
[2] Cantor, C.R. and Schimmel, P.R. (1980) Biophysical Chemistry, Vol. II, W.H. Freeman, New York.
[3] Kuwajima, K. (1995) Methods Mol. Biol. 40, 115–135.
[4] Manning, M.C. and Woody, R.W. (1989) Biochemistry 28, 8609–8613.
[5] Chakrabartty, A., Kortemme, T., Padmanabhan, S. and Baldwin, R.L. (1993) Biochemistry 32, 5560–5565.
[6] Toniolo, C., Bonora, G.M., Bavoso, A., Benedetti, E., di Blasio, B., Pavone, V. and Pedone, G. (1983) Biopolymers 22, 205–215.
[7] Prasad, B.V. and Balaram, P. (1984) CRC Crit. Rev. Biochem. 16, 307–348.
[8] Marshall, G.R., Hodgkin, E.E., Langs, D.A., Smith, G.D., Zabrocki, J. and Leplawy, M.T. (1990) Proc. Natl. Acad. Sci. USA 87 32, 487–491.
[9] Basu, G. and Kuki, A. (1992) Biopolymers 32, 61–71.
[10] Piotto, M., Saudek, V. and Sklener, V. (1992) J. Biomol. NMR 2, 661–665.
[11] Bax, A. and Davis, D.G. (1985) J. Magn. Reson. 65, 355–360.
[12] Bothner-By, A.A., Stephens, R.L., Lee, J.M., Warren, C.D. and Jeanloz, R.W. (1984) J. Am. Chem. Soc. 106, 811–813.
[13] Roberts, G.C. (1993) NMR of Macromolecules: A Practical Approach, IRL Press, New York.
[14] Chakrabartty, A., Kortemme, T. and Baldwin, R.L. (1994) Protein Sci. 3, 843–852.
[15] Andersen, N.H., Liu, Z. and Prickett, K.S. (1996) FEBS Lett. 399, 47–52.
[16] Obrecht, D. et al. (1997) Biopolymers 42, 575–626.
[17] Basu, G. and Kuki, A. (1993) Biopolymers 33, 995–1000.
[18] Wuthrich, K. (1986) NMR of Proteins and Nucleic Acids, John Wiley and Sons, New York.
[19] Wishart, D.S., Sykes, B.D. and Richards, F.M. (1992) Biochemistry 31, 1647–1651.
[20] Scholtz, J.M., Marqusee, S., Baldwin, R.L., York, E.J., Stewart, J.M., Santoro, M. and Bolen, D.W. (1991) Proc. Natl. Acad. Sci. USA 88, 2854–2858.
[21] Scholtz, J.M., Barrick, D., York, E.J., Stewart, J.M. and Baldwin, R.L. (1995) Proc. Natl. Acad. Sci. USA 92, 185–189.
[22] Smith, J.S. and Scholtz, J.M. (1996) Biochemistry 35, 7292–7297.
[23] Augspurger, J.D., Bindra, V.A., Scheraga, H.A. and Kuki, A. (1995) Biochemistry 34, 2566–2576.
[24] Lopez, M.M., Chin, D-H., Baldwin, R.L. and Makhatadze, G. (2002) Proteins 99, 1298–1302.
[25] Basu, G., Kitao, A., Hirata, F. and Go, N. (1994) J. Am. Chem. Soc. 116, 6307–6315.
[26] Hummer, G., Garcia, A.E. and Garde, S. (2001) Proteins 42, 77–84.
[27] Oliveberg, M. (1998) Accounts Chem. Res. 31, 765–772.